THE LEO PARTICULATE ENVIRONMENT AS DETERMINED BY LDEF

Thomas H. See[1], Michael E. Zolensky[2], Friedrich Hörz[2], Ronald P. Bernhard[1], Kimberly S. Leago[1], Jack L. Warren[1], Clyde A. Sapp[1], Tammy R. Foster[1], and William H. Kinard[3]

Abstract

The Meteoroid & Debris Special Investigation Group has been studying the low-Earth orbit particulate environment by examining and documenting impact craters that occurred on the Long Duration Exposure Facility (LDEF) during its 5.7 year stay in orbit.

Introduction

Placed in low-Earth orbit (LEO) by *Challenger* in April 1984, and retrieved by *Columbia* in January 1990, the Long Duration Exposure Facility (LDEF) was a 14-faced (12 sided cylinder and two ends), gravity-stabilized spacecraft that was host to 57 individual scientific experiments. Numerous experiments were designed to characterize various aspects of the meteoroid and orbital-debris environment during the nominal nine month mission. However, as a result of LDEF's unexpectedly long exposure time (5.7 years) and the heightened awareness of the threat of collisions with man-made debris, it was decided to utilize the entire spacecraft as a meteoroid and orbital-debris detector. The Meteoroid & Debris Special Investigation Group (M&D SIG) was organized to achieve this end.

The gravity-gradient stabilization of LDEF (*i.e.,* the same general surface pointed into the velocity vector during the entire mission) and the large exposed surface area (~130 m^2) provided unique information concerning the LEO particulate environment and associated directionality effects for both natural and man-made particles, and the ability to

[1]Lockheed - ESC, C23, 2400 NASA Road 1, Houston, Texas 77058; [2]SN, NASA / Johnson Space Center, Houston, Texas 77058; [3]404, NASA / Langley Research Center, Hampton, Virginia 23665.

refine model-dependent estimates of the velocities of heliocentric particles (*e.g.,* Zook, 1992).

Among the major goals of the M&D SIG were (1) the documentation of the impact record of the entire LDEF, (2) characterization of the LEO particulate environment, and (3) the dissemination of this information, primarily to those interested in the collisional hazard represented by these particles. As a major step toward the accomplishment of these goals, the M&D SIG (1) prepared a publication (See *et al.,* 1990) describing all observations of impact features made during LDEF's deintegration at the Kennedy Space Center (KSC), (2) continues more detailed examination and documentation of impact features on LDEF hardware (*e.g.,* Zolensky *et al.,* 1991; See *et al.,* 1993, 1994*)*, and (3) is archiving all of this data, as well as similar information provided by LDEF Principal Investigators (PI's) (*e.g.,* Bernhard *et al.,* 1993a; Humes, 1992), in a public-domain database, which is maintained at the Johnson Space Center (JSC) in Houston, Texas. This database constitutes the most detailed account of the current LEO particulate environment and will guide additional in-situ investigations of natural and man-made debris in the near-Earth environment. As the orbital-debris population is expected to increase, the LDEF data provide an accurate historical record for the period of 1984-1990 against which future measurements of the debris population can be compared.

Following the deintegration of LDEF at KSC, most subsequent M&D SIG activities have been conducted at JSC, where NASA's Planetary Materials Program maintains its lunar rock, meteorite, and cosmic-dust collections. These long-term curatorial systems provided a ready-made infrastructure for the curation and additional analysis of LDEF samples, the generation and maintenance of an active database, and the allocation and shipment of samples to a wider user community. This report briefly summarizes a cross-section of continuing efforts of the M&D SIG.

3-D Stereo Images

During the four-month deintegration of LDEF at KSC, the M&D SIG generated approximately 4,500 digital, color stereo-image pairs of impact-related features, predominantly craters and penetrations, from the various space-exposed surfaces. Currently these images are being processed at JSC to yield more accurate feature information (*e.g.,* crater depth and diameter with respect to the original target surface). An earlier paper (See *et al.,* 1993) describes the theory and practice of determining this 3-dimensional information from stereo imagery, while a second paper (Sapp *et al.,* 1993) describes some of the problems and solutions encountered during development of the algorithm.

M&D SIG Database

The LDEF M&D database consists of five data tables containing information on (1) the size, type, location, and characteristics of all features documented at KSC and JSC; (2) digitized, color, stereo imaging of all *large* impact features (*i.e.,* craters ≥500 μm in diameter and penetrations ≥300 μm in diameter); and (3) an inventory of all LDEF hardware that is presently archived at JSC. Approximately 4,500 large features were identified during the disassembly of the spacecraft at KSC, and an additional 4,500 or so *smaller* features (*i.e.,* <500 and <300 μm diameter craters and penetrations, respectively) have subsequently been identified and cataloged at JSC. The database also contains limited amounts of information submitted by members of the LDEF PI community; our goal is to include *all* PI data in this database.

Copies of the digitized, color, stereo images are also archived at JSC, although these images are not stored on-line because of the large amount of disk space required. However, the database contains the image filenames (left and right) and the removable disk designation on which each image resides. These images can be made available for downloading at the user's request. In addition, the M&D SIG will be transferring these images to standard CD-ROM (CDR-74 format; ISO-9660) for distribution to interested workers.

Data Tables

The five data tables within the M&D database are (1) Primary Surfaces, (2) Features, (3) Cores, (4) Digital Images, and (5) Allocation History. The Primary Surfaces, Cores, and Allocation History tables are primarily used for tracking samples controlled by JSC, although they do contain other information about the nature of the samples. The Features table represents the focus of the database and contains one record for every feature that has been identified either at KSC, JSC, or by contributing investigators. The Digital Images table represents an index for retrieving digitized images of a feature, when such images exist.

Sample-Numbering Scheme

The feature numbers recorded in the database represent a combination of the surface identifier (ID) and a unique feature number for that surface. The surface ID consists of four parts: the LDEF Bay and Row number, the component type, the component number, and an individual feature number. The bay and row numbers are the same as those initially assigned to the satellite grids (see Figure 1 and See *et al.,* 1990). The component type is a one-letter code which translates to a particular piece of hardware (*e.g.,* “C” for clamps). The component number is a sequential number assigned to

differentiate separate pieces of the same component type taken from the same bay and row.

Cores, which represent features that have been removed from a surface with part of the surrounding substrate, are numbered sequentially as they are removed, regardless of the surface number. All cores taken from LDEF are prefixed with the characters “LD-” to differentiate LDEF cores from those taken from other spacecraft.

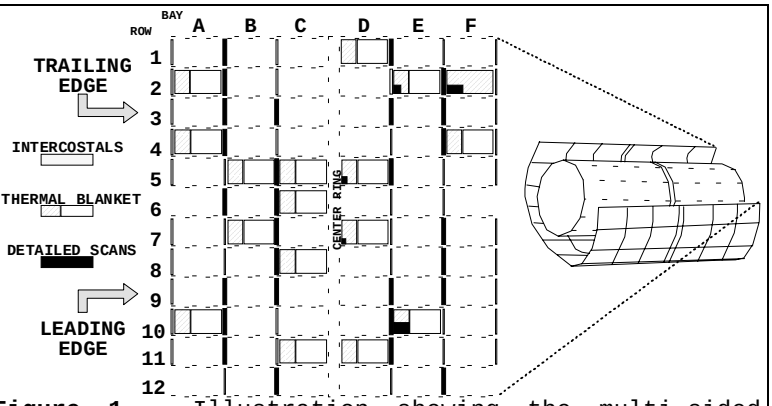

Figure 1. Illustration showing the multi-sided nature of the LDEF spacecraft and associated numbering scheme. The Earth- (G) and space-facing ends (H) would be to the left and right, respectively, in this illustration. Sixty eight, of a possible 72 peripheral intercostals reside at JSC and are being scanned in detail for craters <500 μm in diameter; the results of these detailed scans on 27 intercostals are included in this report. One third of all thermal blankets also reside at JSC.

Impact Damage

A detailed discussion on the resulting impact damage to all material types flown on LDEF is beyond the scope of this contribution and will only be summarized here. More detailed discussions on this topic can be found in See *et al.* (1990) and Allbrooks and Atkinson (1992), the latter of which contains numerous color photographs which show the damage resulting from impacts into many of the various materials flown on LDEF.

LDEF exposed ~130 m^2 of surface area to the LEO particulate environment. The types of materials flown on LDEF can be grouped into five major categories: (1) metals, (2) glasses and other crystalline samples, (3) polymers, (4) composites, and (5) multi-layered thermal blankets and other multi-layered structures.

Metals

Approximately 75 percent (*i.e.,* ~100 m^2) of the exposed surface area on LDEF consisted of diverse aluminum alloys, either uncoated, anodized, or painted. Most craters identified in uncoated metal surfaces were symmetrical and possessed raised rims; only a small percentage exhibited asymmetric shapes or petaled rims, or were elliptical. A few, clearly identifiable multi-cratering events were also found on such surfaces. The largest crater (~5.25 mm in diameter) was located on a forward-facing aluminum frame

located on the space-facing end (facing away from Earth) of LDEF.

Penetrations through thin metal surfaces, and a few large impacts through 1 mm thick aluminum sheet metal, had the general symmetrical hole and rim shapes common to such events. Impacts >0.5 mm in diameter into painted metal surfaces generally produced associated spall zones in the paint which extended for several crater diameters around the crater.

Glasses

Several square meters of surface area on LDEF were covered with glass-encased solar cells or covers/windows, metal-oxide-silicon (MOS) capacitor-type detectors, germanium crystal wafers, and hundreds of small glass and crystalline samples. The morphology of impacts into and through glass and crystalline surfaces was dependent on the physical properties of the individual material. Such features had several, and frequently all of the following characteristics (1) rims, (2) spall zones, (3) fracture zones, some of which extended large distances from the impact point. The extent of the spall and fracture zones, and the presence or absence of a rim were the major differences among features in glass and crystalline surfaces.

Polymers

Seventeen experiment trays were covered by ~200 μm thick thermal blankets which consisted of an outer, space-facing layer of FEP Teflon (~120 μm thick) backed by a thin layer of vapor-deposited silver/inconel (~200 to 300 Å), which was backed by DC1200 primer and Chemglaze Z306 black conductive paint (~80 to 100 μm thick). Impacts into these blankets produced delamination zones which commonly extended tens of penetration-hole or crater diameters, separating the Teflon layer from the silver/inconel and paint coatings. Penetration holes were often surrounded by one or more, whole or partial, colored rings which varied dramatically in size and color.

Impacts into laminated polymeric films, such as Kapton, produced craters and penetration holes with the general structure described above, but also had areas of delamination which appeared as bubbles between layers. Reinforced layered plastics had less extensive delamination zones, and frayed fibers were often noted overlapping the holes in the polymer.

Composite Structures

Several experiment trays exposed various amounts of composite surfaces which were constructed from several layers of carbon, glass, and/or Kevlar woven fibers, with layers being laminated together with resin binders. Impact-induced damage of these structures generally took the form of broken fibers with missing binder material from the affected volume.

Remnant fibers often could be found extending over the area of missing or excavated binder material. In some cases the diameter of the affected volume increased with depth. Spall zones were commonly visible around impacts. The spall zones, which generally extended a few crater diameters, represented areas where binder material had been ejected. Delamination-type zones were present around many large impacts in horizontally lapped composite structures. These areas usually extended a few crater diameters beyond the spall zone, and were most easily identified in translucent materials.

Multi-layer Thermal Blankets and Structures

Several square meters were covered with multi-layer thermal blankets (MTB) or other multi-layered surfaces, sometimes separated by Dacron netting. Large impacts into MTBs produced a "normal" penetration hole in the exterior layer, followed by successively larger holes in subsequent layers caused by the expanding debris cloud. Shadow images of the Dacron netting were present on impact-affected areas of many of the subsurface films in the MTBs. Secondary craters and penetration holes often surrounded this shadowed netting image.

Impacts into beta-cloth blanket material were similar to penetrations in the fibrous composites, with the major visible damage being the rupture of the fibers. Impacts into multi-layer structures produced penetrations through varying numbers of layers of the laminated structure. A variety of delamination and spall zones were present around several of the large impact sites.

Particle Flux

LDEF's structural frame consisted of two major components, termed *longerons* and *intercostals*, which offer the opportunity to characterize the impact record on a uniform material type (*i.e.,* 6061-T6 aluminum) that was exposed in all LDEF pointing directions. Longerons (each about 3 m long) occupied the position between rows. Intercostals (each about 1 m long) ran perpendicular to the longerons and were located to the side of each experiment bay (see Figure 1). The M&D SIG has acquired 68 of the 72 peripheral intercostals and is presently scanning these frame members to document the crater-size frequency down to ~50 μm diameter; each intercostal exposed ~0.06 m^2 to the LEO particulate environment. At the time of this writing, the M&D SIG has such data for 27 intercostals, at least two from each of the 12 rows (Figure 1).

The cumulative size-frequency distribution of craters on these intercostals can be seen in Figures 2a & b. Figure 2a illustrates the size-frequency distributions for the 27 intercostals examined to date. As expected (Zook, 1992;

Kessler, 1992), the highest cratering rates were observed in the forward-facing directions (*i.e.,* Rows 8, 9 and 10), while the lowest were found in association with the rearward-facing surfaces (*i.e.,* Rows 2, 3 and 4). In general, the slopes of these curves are very similar, suggesting that the overall ratio of large to small particles remains relatively constant, regardless of pointing direction. An exception to this relationship can be seen for Row 7. Intercostal F07F02 possessed an unusually high density of craters <30 μm in diameter. In fact, the number of craters <30 μm in diameter on F07F02 is more than three times greater than for the leading-edge intercostals. Furthermore, this intercostal possesses a factor of 2.8 more craters, and more than 10 times the number of <30 μm diameter craters than does C07F02, another Row 7 intercostal. D. Humes (personal communications, 1992) examined some of the hardware associated with his experiment trays located on either side of intercostal F07F02, and found a crater density that was actually slightly higher than that determined for F07F02.

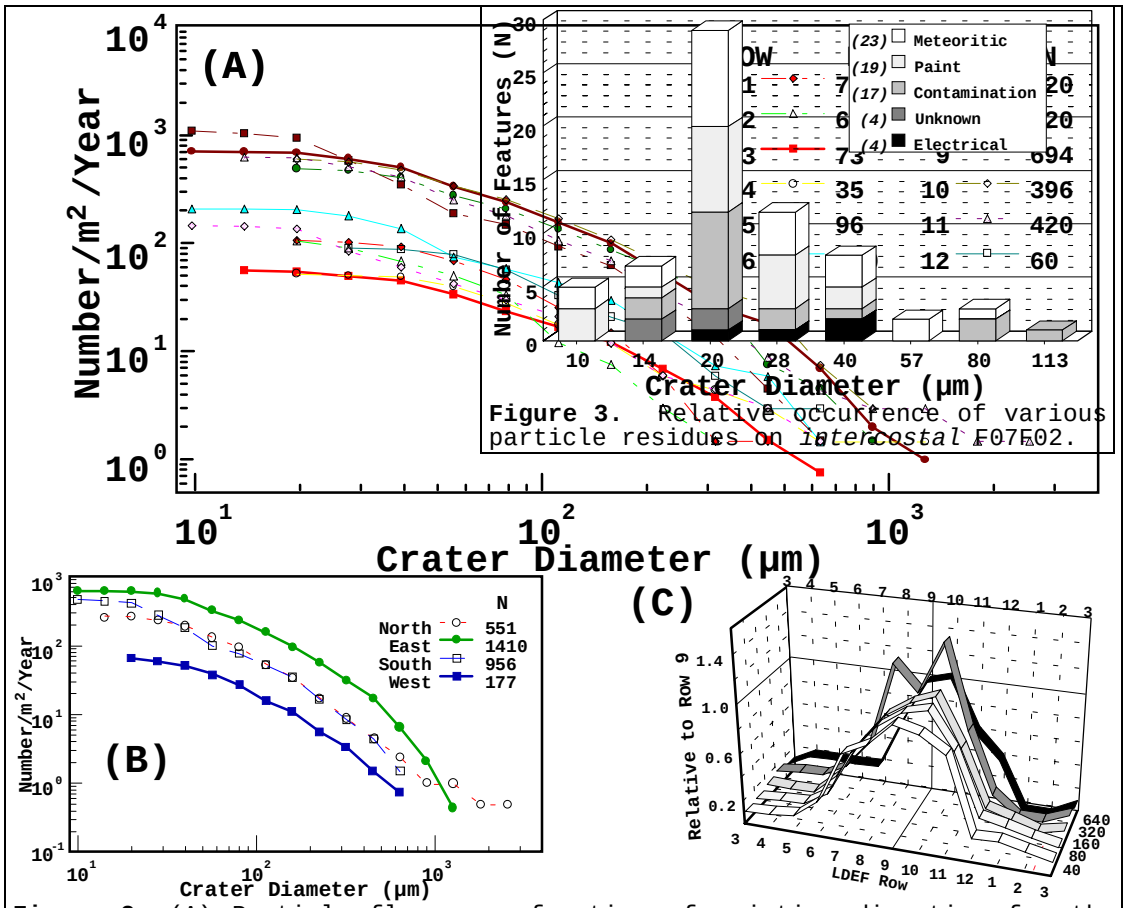

Figure 3. Relative occurrence of various particle residues on *intercostal* F07F02.

Figure 2. (A) Particle flux as a function of pointing direction for the LDEF *intercostal* frame members; Row 9 was the leading-edge or velocity-vector pointing direction. (B) Average particle flux for the four major pointing directions of LDEF (North equals the average flux of Row 11, 12, 1, etc.) (C) Relative impact frequency for selected craters diameters with respect to Row 9. In Figures 2a & 2b N equals the number of craters associated with each line.

Preliminary chemical analysis of ~10% of the impacts on F07F02 reveals a modest increase in the relative number of paint-type residue as compared to residues found on tray clamps and the gold surfaces from experiment A0187-1 (Bernhard *et al.*, 1993a, b). However, LDEF does not possess any protrusions or other geometry that is conducive to the local generation of a large number of secondary ejecta particles, a process that accounts for local variations in the density of small craters on Solar Maximum satellite surfaces (Warren *et al.*, 1988). Thus, the source of these numerous small particles remains a mystery at this time.

Figure 2b depicts the average crater frequencies for the four main LDEF pointing directions (*i.e.*, 12 [north], 9 [east or forward-facing], 6 [south] and 3 [west or rear-facing]). Each curve represents the average of the main row from each direction plus the rows on either side (*i.e.*, west represents the average of Rows 2, 3 and 4). Such a plot is useful in revealing the overall trends associated with each of these

See

four pointing directions. As would be expected from Figure 2a, the forward-facing rows have the highest cratering frequency, while the rearward-facing rows exhibit the lowest. The elevated flux below 30 μm for the southern-facing rows is due to intercostal F07F02 (see above).

Figure 2c depicts the relative production rates (normalized to Row 9) for five selected crater-diameter ranges. This figure shows that the ratio of the impact rate for the leading edge to that on the trailing edge varies as a function of the crater diameter. Comparing Rows 9 and 3, the ratio is 11:1 for the smallest craters in this plot (*i.e.*, ≥ 40 to <57 μm in diameter). In general, the leading-edge:trailing-edge ratio decreases as feature size increases (~10:1, 8:1, 7:1, and 9:1 for ≥80 to 113, ≥160 to 226, ≥320 to 453, and ≥640 to 905, respectively). Comparing the averages (Figure 2b) of the east- and west-facing directions, the ratio for all feature sizes is 9:1.

Impactor Composition

Of the more than 1,100 craters analyzed at JSC by SEM-EDX techniques, about half contain no detectable residue (Figure 4), implying loss of impactor material by ejection or complete vaporization. It is extremely important to note that aluminum projectiles cannot be detected on aluminum substrates (*i.e.,* a significant fraction of the "unknown" craters for experiment tray A11 and the clamps [Figure 4a and c, respectively] could be the result of aluminum projectiles).

Of the identifiable residues from the *Chemistry of Micrometeoroids Experiment* and the tray clamps, natural particles dominate at all crater sizes >10 μm (*i.e.,* ~44%, ~30% and ~30% for A11, A03 and the clamps, respectively). Orbital-debris was identified in ~12%, ~14% and ~10% of the craters on the same surfaces, respectively. Some of these residues have been subdivided into various sub-classes. Chondritic compositions are the most common among the natural impactors (67%), followed by monomineralic, mafic-silicate compositions (28%), and Fe-Ni rich sulfides (~4%). Of interest is the fact that ~30% of all identifiable residues on the gold collectors were caused by man-made debris such as aluminum (~85%), paint flakes (~4%), and other dis-integrated, structural and electronic components (~11%).

Prior to LDEF, it was believed that trailing-edge surfaces would not experience impacts by any man-made debris (Kessler, 1992). The discovery of such impacts on LDEF forced revisions of the various models of the LEO particulate environment. Kessler (1992) concluded that a substantial population of debris must exist in highly elliptic, low-inclination orbits, such as those that are typically occupied by transfer vehicles of geosynchronous payloads.

References

Allbrooks, M.K. and Atkinson, D., 1992, *The Magnitude of Impact Damage on LDEF Materials*, M&D SIG Publication, 82 pp. Available from LDEF Project Office, 404 NASA/LaRC, Hampton, VA. 23665 or from Mike Zolensky, SN2, NASA/JSC, Houston, TX. 77058.

Bernhard, R.P., See, T.H., and Hörz, F., 1993a, Projectile Compositions and Modal Frequencies on the "Chemistry of Micrometeoroids" LDEF Experiment, *LDEF - 69 Months In Space. Second Post-Retrieval Symposium, NASA CP-3194*, p. 551-574.

Bernhard, R.P. and Zolensky, M.E., 1993b, Analysis of Impactor Residues in Tray Clamps from the Long Duration Exposure Facility, Part 1: Clamps from Bay "A" of the Satellite, *NASA Tech. Memo. #104759*, 194 pp.

Humes, D., 1992, Large Craters on the Meteoroid and Space Debris Impact Experiment, *LDEF - 69 Months In Space. First Post-Retrieval Symposium, NASA CP-3134*, p. 399-418.

Kessler, D.J., 1993, Origin of Orbital-Debris Impacts on LDEF's Trailing Edge, *LDEF-69 Months in Space, Second Post Retrieval Symposium,. NASA CP-3194*, p. 585-593.

See, T.H., Allbrooks, M.K., Atkinson, D., Simon, C., and Zolensky, M.E., 1990, *Meteoroid and Debris Impact Features Documented on the Long Duration Exposure Facility: A Preliminary Report*, NASA/JSC Publication 24608, Planetary Sciences Branch Publication 84, 586 pp.

See, T.H., Allbrooks, M.K., Atkinson, D.R., Sapp, C.A., Simon, C.G., and Zolensky, M.E., 1992, Meteoroid & Debris Special Investigation Group: Data Acquisition Procedures. *LDEF - 69 Months In Space. First Post-Retrieval Symposium, NASA CP-3134*, p. 459-476.

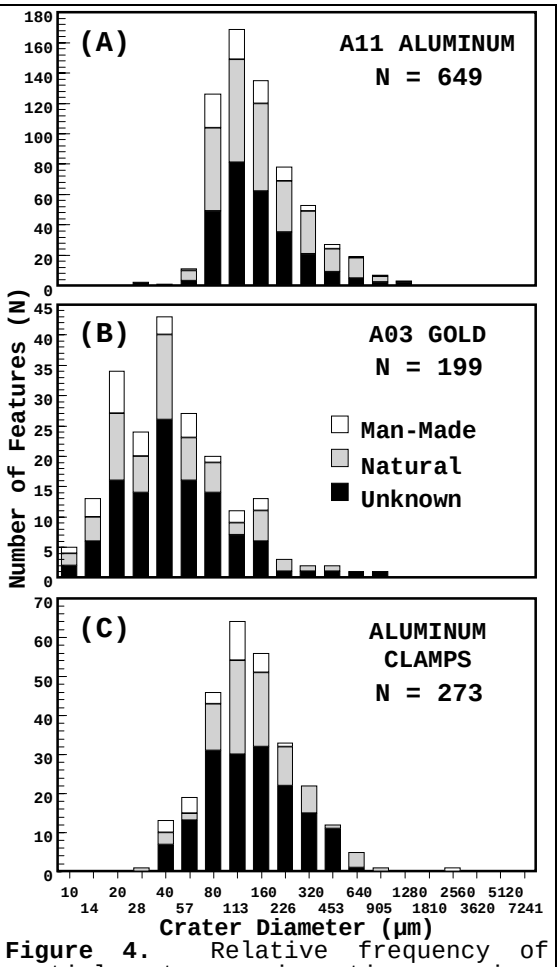

Figure 4. Relative frequency of particle types impacting various LDEF surfaces. Aluminum (A) and Gold (B) collectors of the *Chemistry of Micrometeoroids Experiment*, located in forward-facing and trailing-edge directions, respectively. (C) Experiment-tray clamps from Bays A & B for all 12 peripheral LDEF rows.

See, T.H., Mack, K.S., Warren, J.L., Zolensky, M.E., and Zook, H.A., 1993, Continued Investigation of LDEF's Frame and Thermal Blankets by the Meteoroid & Debris Special Investigation Group, *LDEF - 69 Months In Space. Second Post-Retrieval Symposium, NASA CP-3194*, p. 313-324.

See, T.H., Warren, J.L., Leago, K.S., and Zolensky, M.E., 1993, Particle Flux as a Function of Pointing Direction as Determined from LDEF's Structural-Frame Components by the Meteoroid & Debris Special Investigation Group (abstract), *Third LDEF Post-Ret. Sym.*, in press.

Sapp, C.A., See, T.H., and Zolensky, M.E., 1993, 3-D Crater Analysis of LDEF Impact Features From Stereo Imagery, *LDEF - 69 Months In Space. Second Post-Retrieval Symposium, NASA CP-3194*, p. 339-346.

Warren, J.L., Zook, H.A., Allton, J.H., Clanton, U.S., Dardano, C.B., Holder, J.A., Marlow, R.R., Schultz, R.A., Watts, L.A., and Wentworth, S.J., 1989, The Detection and Observation of Meteoroid and Space Debris Impact Features on the Solar Max Satellite, *Proc. Lunar Planet. Sci. Conf. 19th*, p. 641-658.

Zolensky, M., Atkinson, D., See, T.H., Allbrooks, M., Simon, C., Finckenor, and Warren, J., 1991, Meteoroid and Orbital Debris Record of the Long Duration Exposure Facility's Frame*, J. Spacecraft and Rockets, 28, #2*, p. 204-209.

Zook, H., 1992, Deriving the Velocity Distribution of Meteoroids from the Measured Meteoroid Impact Directionality on the Various LDEF Surfaces, *LDEF - 69 Months In Space. First Post-Retrieval Symposium, NASA CP-3134*, p. 569-580.